Hindawi
Advances in Civil Engineering
Volume 2019, Article ID 6186748, 12 pages
https://doi.org/10.1155/2019/6186748

Research Article

Vertical Load and Settlement at the Foot of Steel Rib with the Support of Feet-Lock Pipe in Soft Ground Tunnel

Lijun Chen, Jianxun Chen, Yanbin Luo, Yao Li, and Taotao Hu

School of Highway, Chang'an University, Xi'an 710064, Shannxi Province, China

Correspondence should be addressed to Jianxun Chen; chenjx1969@chd.edu.cn

Received 19 August 2018; Accepted 2 January 2019; Published 3 February 2019

Academic Editor: Farhad Aslani

In soft ground tunnels, feet-lock pipes have been widely used to decrease the concentration of load and settlement at the foot of steel ribs. This paper presents an analytical method to predict the vertical load and settlement at the foot of steel ribs with the support of the feet-lock pipe. First, the mechanical model of a steel rib and feet-lock pipe combined structure involving the ground reaction at the foot was proposed. In this model, the deformation compatibility among the steel rib, the feet-lock pipe, and the ground at the tunnel foot were considered, and an elastic foundation beam model with double parameter for the feet-lock pipe was proposed. Then, based on the proposed mechanical model, the analytical equations for predicting the vertical load and settlement at the foot of the steel rib were derived using structural analysis and beam theory on elastic foundation. The predicted vertical loads and settlements were validated by comparing with the results of field measurements and the Winkler foundation beam model for the feet-lock pipe, and the results show that the feet-lock pipe can effectively reduce the load acting on the ground, where the steel rib was installed, and finally improve the stability of the tunnel structure.

1. Introduction

A steel rib bears most earth pressure in the primary support system and controls the early stage deformation of a tunnel in soft ground. Its stability directly affects the stability of the tunnel structure. While tunneling using a partial excavation method, it often encounters the subsidence of the steel rib due to the excessive vertical load or small bearing capacity of the ground at the tunnel foot (Figure 1), which can directly lead to a series of settlement problems [1–3]. Therefore, it is very important to control the foot settlement by taking various auxiliary measures, such as the high-pressure jet grouting column [4, 5], foot bolt ore side pile [6, 7], and enlarged tunnel foot [1]. In recent years, one effective measure in this situation is adopting the feet-lock pipe. The feet-lock pipe is composed of steel pipes or bolts that are inserted in the ground near the tunnel foot. Its near-end is firmly welded to the foot of the steel rib (Figure 2). Once the feet-lock pipe is installed, the vertical load acting on the ground at the tunnel foot can be transferred to the feet-lock pipe, and the foot settlement of the steel rib can be reduced. In engineering practice, the feet-lock pipe is widely used when the steel rib cannot be directly placed on a solid ground. In addition, the feet-lock pipe can be used as presupport for the excavation below the upper section.

The application of the feet-lock pipe has been reported in numerous studies [8–13]. The supporting mechanism and mechanical characteristics of the feet-lock pipe have also been studied by many research studies in field tests, laboratory experiments [14–16], numerical modeling [2, 3, 17, 18], and analytical studies [11, 16]. In these research results, it can be concluded that the feet-lock pipe mainly exerts shear and bending resistance to prevent the foot settlements of the tunnel, and it has the different action mechanisms with the rock bolt, which mainly exerts tensile strength.

Although the feet-lock pipe helps decrease the vertical load and settlement at the foot of steel ribs, it is still necessary to check the ground stability at the foot in soft ground, and to ensure the foot settlement is controlled in an allowable range. In recent years, only few researchers studied the ground stability at the foot of the steel rib with the support of

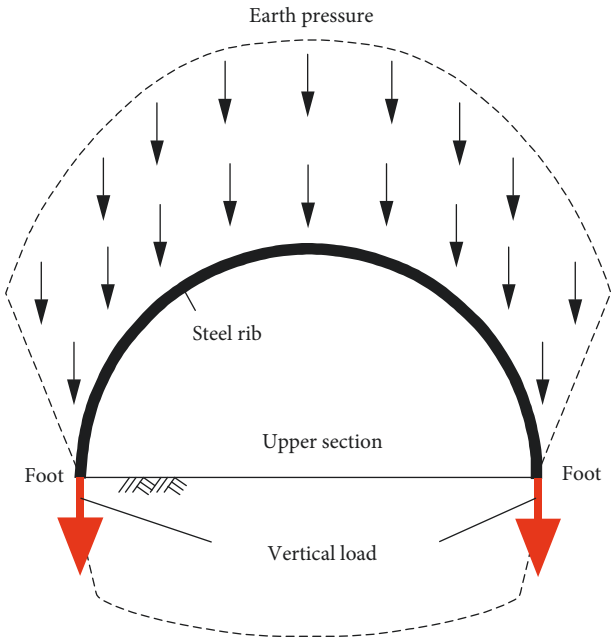

Figure 1: Steel ribs without the support of the feet-lock pipe.

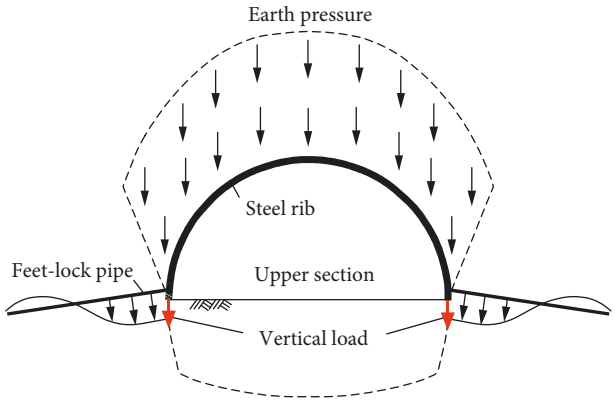

Figure 2: Steel ribs with the support of the feet-lock pipe.

the feet-lock pipe [19, 20]. In order to evaluate the ground stability at the tunnel foot, Wu et al. [19] and Tan et al. [20] derived the formulas of the vertical load at the tunnel foot based on the mechanical model of primary support with the support of the feet-lock pipe. In these works, the vertical loads were considered to be the difference between vertical earth pressure acted on the tunnel support and vertical bearing capacity of the feet-lock pipe. Because the deformation compatibility among the steel rib, the feet-lock pipe, and the ground at the tunnel foot were ignored, the calculated values were only the minimum of the vertical loads. Hence, it is dangerous to use these values to evaluate the ground stability at the tunnel foot. On the contrary, the feet-lock pipe was usually modeled as a beam on the Winkler foundation [11, 19, 20], which modeled the ground as a series of independent springs and neglected the continuity of ground displacements, namely, the shear resistance of the ground. As a result, the calculated vertical loads at the tunnel foot were far from actual vertical loads. In addition, in previous work, the settlement and vertical load at the foot of the steel rib with the support of the feet-lock pipe cannot be obtained at the same time; for instance, the foot settlement cannot be obtained using the method of Wu et al. [19] and Tan et al. [20], while the vertical load at the foot of the steel rib cannot be obtained using the method of Chen et al. [11].

In this study, in order to reasonably predict the vertical load and settlement at the foot of the steel rib with the support of the feet-lock pipe, the deformation compatibility among the steel rib, the feet-lock pipe, and the ground at the tunnel foot were considered in the proposed mechanical model. Besides, an elastic foundation beam model with double parameter for the feet-lock pipe was established to reflect the shear resistance of the ground. By using structural analysis and beam theory on elastic foundation, the calculation formulas of the vertical load and foot settlement were derived at the same time, and the predictions were compared with the field measurements and those of the Winkler model of the feet-lock pipe to validate the presented method.

2. Problem Description and Modeling

The problem proposed in this paper deals with the stability evaluation of the ground at the foot of the steel rib with the support of the feet-lock pipe in a soft ground tunnel when tunneling using a partial excavation method. The problem is to be solved by calculating the vertical load and foot settlement of the steel rib with the support of the feet-lock pipe based on an ideal mechanical model. In this model, the following assumptions were made: (i) the feet-lock pipes are installed symmetrically on both sides of the steel rib. (ii) Due to the poor combination of the steel frame and shotcrete, the adhesion is small, and the gap between the steel frame and the surrounding rock is difficult to be filled with the shotcrete. The steel rib can be designed to bear the earth pressure alone in the early stage after the tunnel excavation. The vertical earth pressure acting on the steel rib can be regarded as uniformly distributed. The lateral earth pressure can be regarded as a trapezoidal load (Figure 3(a)). (iii) The feet-lock pipe mainly exerts its effect of shear and bending resistance to prevent the settlement of the steel rib. Its near-end is mainly subjected to the lateral loads, such as the shear force and bending moment transferred from the foot of the steel rib. Under the action of the shear force and bending moment, the feet-lock pipe can be analyzed as a beam or extended foot of the steel rib on elastic foundation (Figure 3(b)). (iv) The near-end of the feet-lock pipe is usually located about 30~50 cm from the foot of the steel rib. Because of the structural integrity between steel rib and feet-lock pipe, the support reaction of the steel rib along the axis of the feet-lock pipe can be completely supplied by the ground near the side wall, so that the steel rib can always maintain stability even when there is no side resistance and bottom resistance of the feet-lock pipe. Therefore, it is assumed that the feet-lock pipe is only subjected to above lateral loads. (v) The upper-bench ground at the foot of the steel rib can be modeled as a vertical reaction spring that sustains the vertical load (Figure 3(c)). Thus, the supporting conditions of the steel rib at the foot can be considered as a

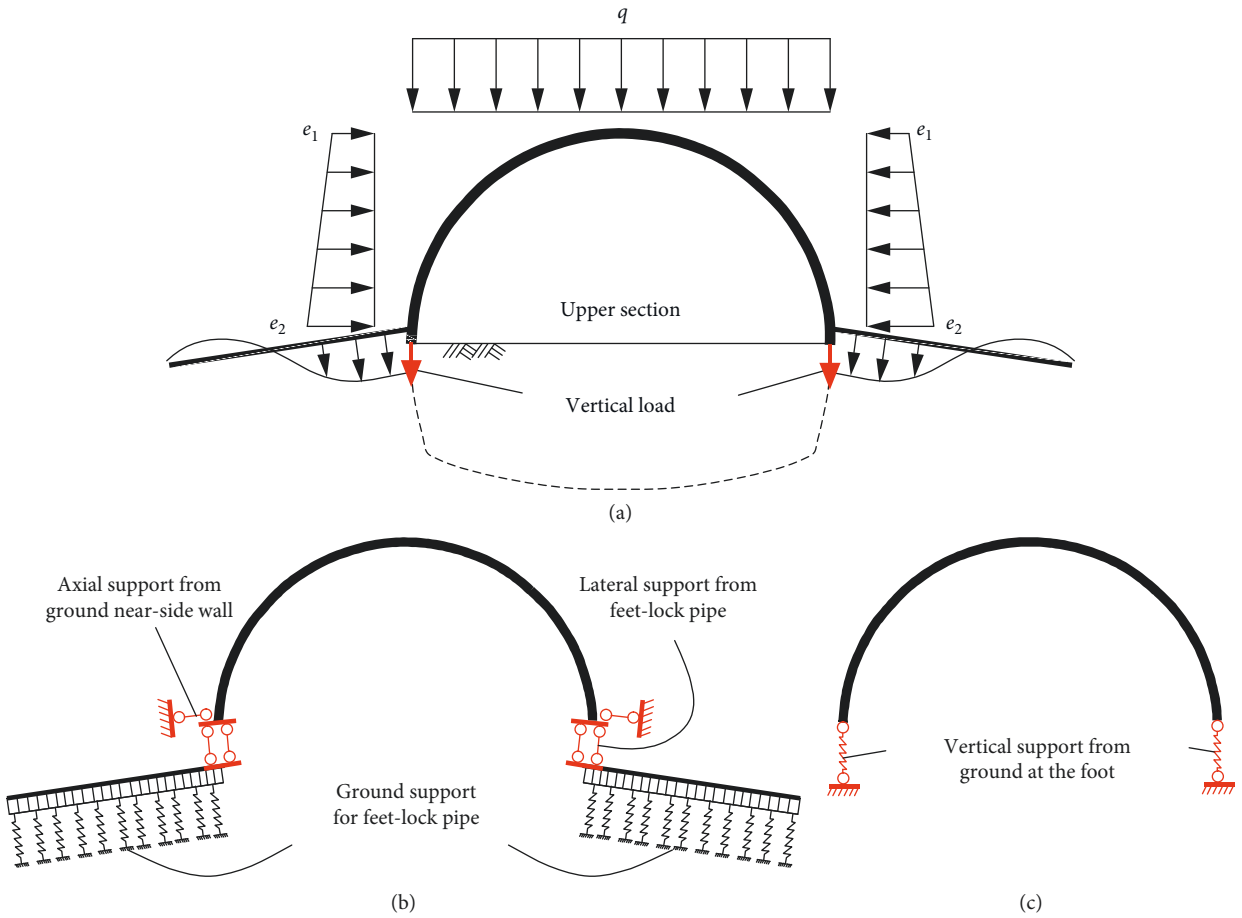

FIGURE 3: Ideal mechanical model of the steel rib, feet-lock pipe, and ground: (a) earth pressure acting on the steel rib; (b) ideal support between steel rib and feet-lock pipe; (c) ideal support between steel rib and upper-bench ground.

superposition of the two cases showed in Figures 3(b) and 3(c). With the above assumptions, the mechanical model for the vertical load and settlement at the foot of the steel rib with the support of the feet-lock pipe was established.

3. Derivation of Vertical Load and Foot Settlement

In the proposed mechanical model, a fixed arch and a beam on elastic foundation compose the combined structure of the steel rib and the feet-lock pipe as shown in Figure 4. There are three unknown forces that need to be determined, namely, the bending moment X_1, axial force X_2 on the crown, and the vertical foundation reaction X_3 at the foot. The force method is one of the first available to determine the unknown forces. Once these forces are determined, the remaining reactive forces on the structure can be determined by satisfying the equilibrium requirements.

3.1. Mechanical Analysis of Steel Ribs. Figure 5 shows the primary structure of steel ribs analyzed by the force method. Assuming all the forces and displacements are shown in the positive direction. According to the deformation compatibility at the crown cross section and the foot cross section of the steel rib, the relative rotational angle and relative horizontal displacement at the crown section of the steel rib are zero, and the vertical displacement at the foot section of the steel rib equals to the compression deformation of the upper-bench ground. Accordingly, we can get

$$\left.\begin{aligned} \delta_{11}X_1 + \delta_{12}X_2 + \Delta_{1p} + \beta_0 &= 0 \\ \delta_{21}X_1 + \delta_{22}X_2 + \Delta_{2p} + u_0 + f\beta_0 &= 0 \\ X_1\nu_1 + X_2(\nu_2 + f\nu_1) + X_3\nu_3 + \nu_p &= X_3/(K_f A_f) \end{aligned}\right\}, \tag{1}$$

where

$$\begin{aligned} \beta_0 &= X_1\beta_1 + X_2(\beta_2 + f\beta_1) + X_3\beta_3 + \beta_p, \\ u_0 &= X_1u_1 + X_2(u_2 + fu_1) + X_3u_3 + u_p, \end{aligned} \tag{2}$$

K_f is the coefficient of foundation reaction at the foot of the steel rib (N/m^3), A_f is the contact area between the foot of the steel rib and the ground (m^2), f is the height of the upper section (m), δ_{ik} $(i, k = 1, 2)$ are, respectively, the crown displacements along the directions of X_i caused by X_k $(X_k = 1)$ in the case that the feet of the steel rib are rigidly constrained, Δ_{ip} $(i = 1, 2)$ are the crown displacements along the directions of X_i caused by the earth pressures in the case that the feet of the steel rib are rigidly constrained. The above crown displacements are given as follows:

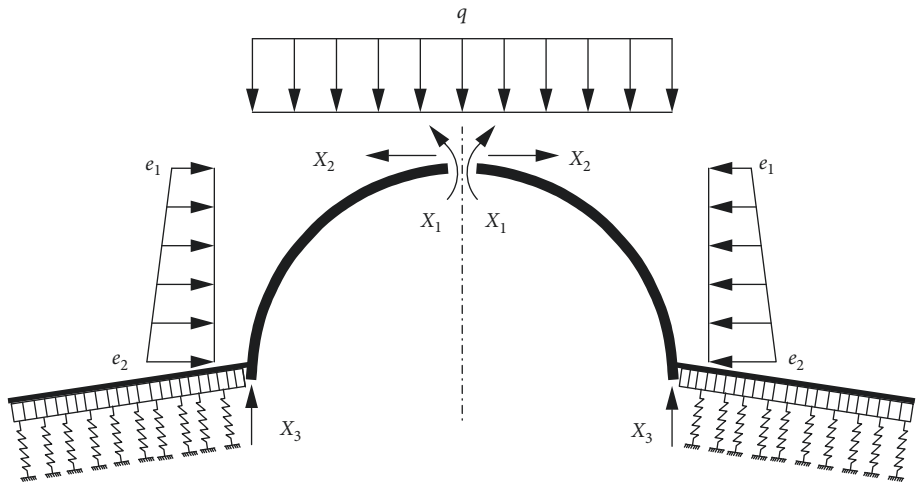

Figure 4: Mechanical model of the steel rib with the support of the feet-lock pipe.

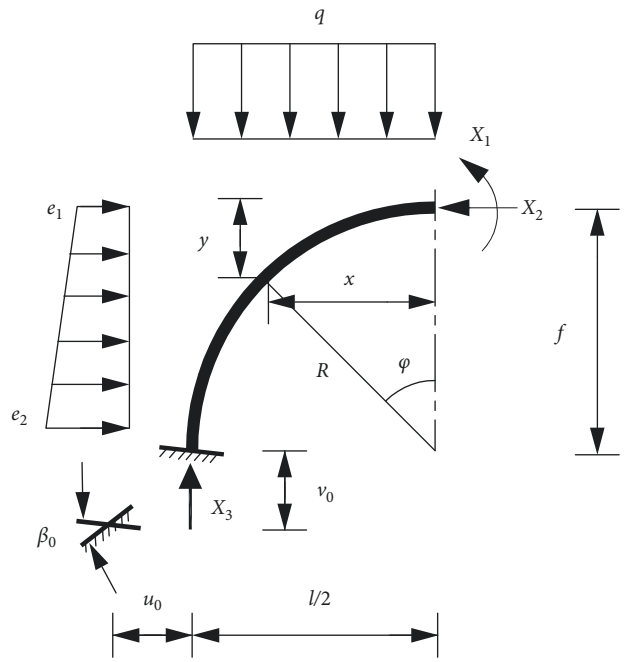

Figure 5: Mechanical analysis of the steel rib by the force method.

$$\delta_{11} = \int_0^{\varphi_m} \frac{R}{E_a I_a} d\varphi = \frac{R\varphi_m}{E_a I_a}, \tag{3}$$

$$\delta_{12} = \delta_{21} = \int_0^{\varphi_m} \frac{R^2(1-\cos\varphi)}{E_a I_a} d\varphi = \frac{R^2}{E_a I_a}(\varphi_m - \sin\varphi_m), \tag{4}$$

$$\delta_{22} = \int_0^{\varphi_m} \frac{R^3(1-\cos\varphi)^2}{E_a I_a} d\varphi = \frac{R^3}{2E_a I_a} \cdot \left(3\varphi_m - 4\sin\varphi_m + \frac{1}{2}\sin(2\varphi_m)\right), \tag{5}$$

$$\begin{aligned}\Delta_{1p} &= -\int_0^{\varphi_m} \frac{qR^3\sin^2\varphi}{2E_a I_a} d\varphi - \int_0^{\varphi_m} \frac{e_1 R^3(1-\cos\varphi)^2}{2E_a I_a} d\varphi \\ &\quad - \int_0^{\varphi_m} \frac{R^4(e_2-e_1)(1-\cos\varphi)^3}{3E_a I_a f} d\varphi \\ &= -\frac{qR^3}{4E_a I_a}\left(\varphi_m - \frac{1}{2}\sin(2\varphi_m)\right) - \frac{e_1 R^3}{2E_a I_a} \\ &\quad \cdot \left(\frac{3}{2}\varphi_m - 2\sin\varphi_m + \frac{1}{4}\sin(2\varphi_m)\right) \\ &\quad - \frac{R^4(e_2-e_1)}{6E_a I_a f} \\ &\quad \cdot \left(\frac{5}{2}\varphi_m - 4\sin\varphi_m + \frac{3}{4}\sin(2\varphi_m) + \frac{1}{3}\sin^3\varphi_m\right),\end{aligned} \tag{6}$$

$$\begin{aligned}\Delta_{2p} &= -\int_0^{\varphi_m} \frac{qR^4(1-\sin\varphi)\sin^2\varphi}{2E_aI_a}d\varphi \\ &\quad -\int_0^{\varphi_m} \frac{e_1R^4(1-\sin\varphi)(1-\cos\varphi)^2}{2E_aI_a}d\varphi \\ &\quad -\int_0^{\varphi_m} \frac{R^5(e_2-e_1)(1-\sin\varphi)(1-\cos\varphi)^3}{3E_aI_af}d\varphi \\ &= -\frac{qR^4}{4E_aI_a}\left(\varphi_m-\frac{1}{2}\sin(2\varphi_m)-\frac{2}{3}\sin^3\varphi_m\right)-\frac{e_1R^4}{2E_aI_a} \\ &\quad \cdot\left(\frac{5}{2}\varphi_m-4\sin\varphi_m+\frac{3}{4}\sin(2\varphi_m)+\frac{1}{3}\sin^3\varphi_m\right) \\ &\quad -\frac{R^5(e_2-e_1)}{6E_aI_af}\left(\frac{35}{8}\varphi_m-8\sin\varphi_m+\frac{7}{4}\sin(2\varphi_m)\right. \\ &\quad \left.+\frac{4}{3}\sin^3\varphi_m+\frac{1}{32}\sin(4\varphi_m)\right),\end{aligned} \tag{7}$$

where

$$\varphi_m = \sin^{-1}\left(\frac{l}{2R}\right), \tag{8}$$

E_aI_a is the bending stiffness of the steel rib, E_a is the Young's modulus of steel (Pa), I_a is the moment of inertia (m^4) of the steel rib, l is the span of the upper section (m), and R is the radius of the steel rib on the upper section (m).

In addition, as shown in Figure 6, u_1, v_1, and β_1 are, respectively, the horizontal displacement, vertical displacement, and rotational angle at the foot section of the steel rib when a unit bending moment is applied to the foot section; u_2, v_2, and β_2 are, respectively, the horizontal displacement, vertical displacement, and rotational angle at the foot section of the steel rib when a unit horizontal force is applied to the foot section; u_3, v_3, and β_3 are, respectively, the horizontal displacement, vertical displacement, and rotational angle at the foot section of the steel rib when a unit vertical force is applied to the foot section; and u_p, v_p, and β_p are, respectively, horizontal displacement, vertical displacement, and rotational angle at the foot section of the steel rib caused by the earth pressures. According to the deformation compatibility condition between steel rib and feet-lock pipe, all above displacements at the foot section are mainly depend on the lateral displacements at the near-end of the feet-lock pipe.

On solving equation (1), the three unknown forces X_1, X_2, and X_3 in Figure 4 can be expressed as follows:

$$\begin{aligned}X_1 &= \frac{\Delta_{X_1}}{\Delta_X}, \\ X_2 &= \frac{\Delta_{X_2}}{\Delta_X}, \\ X_3 &= \frac{\Delta_{X_3}}{\Delta_X},\end{aligned} \tag{9}$$

where

$$\begin{aligned}\Delta_X &= \begin{vmatrix} a_{11} & a_{12} & a_{13} \\ a_{21} & a_{22} & a_{23} \\ a_{31} & a_{32} & a_{33} \end{vmatrix}, \\ \Delta_{X_2} &= \begin{vmatrix} a_{11} & -a_{10} & a_{13} \\ a_{21} & -a_{20} & a_{23} \\ a_{31} & -a_{30} & a_{33} \end{vmatrix}, \\ \Delta_{X_1} &= \begin{vmatrix} -a_{10} & a_{12} & a_{13} \\ -a_{20} & a_{22} & a_{23} \\ -a_{30} & a_{32} & a_{33} \end{vmatrix}, \\ \Delta_{X_3} &= \begin{vmatrix} a_{11} & a_{12} & -a_{10} \\ a_{21} & a_{22} & -a_{20} \\ a_{31} & a_{32} & -a_{30} \end{vmatrix}, \\ a_{11} &= \delta_{11}+\beta_1, \\ a_{12} &= a_{21} = \delta_{12}+\beta_2+f\beta_1, \\ a_{13} &= \beta_3, \\ a_{22} &= \delta_{22}+2f\beta_2+f^2\beta_1+u_2, \\ a_{23} &= f\beta_3+u_3, \\ a_{31} &= v_1, \\ a_{32} &= fv_1+v_2, \\ a_{33} &= v_3-1/(\mathrm{KA}), \\ a_{10} &= \Delta_{1p}+\beta_p, \\ a_{20} &= \Delta_{2p}+u_p+f\beta_p, \\ a_{30} &= v_p.\end{aligned} \tag{10}$$

3.2. Mechanical Analysis of the Feet-Lock Pipe. The near-end of the feet-lock pipe mainly bears the lateral shear load and bending moment applied by the steel rib, as shown in Figure 7. Under the action of the Q_0 and M_0, the feet-lock pipe can be analyzed as a beam on elastic foundation. In order to obtain the lateral displacement and rotation angle of the feet-lock pipe at its near-end, the mechanical model of the feet-lock pipe based on the Pasternak double-parameter foundation is developed with the assumption that the shear stress can be transferred between the foundation springs. Under the shear force Q_0 and bending moment M_0, the foundation reaction of the feet-lock pipe can be expressed as [21]

$$p(x) = KBy(x) - GB\frac{d^2y(x)}{dx^2}, \tag{11}$$

where $p(x)$ is the foundation reaction (N/m), B is the effective width of the feet-lock pipe (m), $y(x)$ is the deflection of the feet-lock pipe, K is the coefficient of the foundation reaction (N/m^3), and G is the shear stiffness of foundation (N/m), which is different from the shear modulus of the foundation material. When G is zero in equation (8), the foundation reaction $p(x)$ corresponds to the well-known equation of the Winkler foundation beam model.

The coefficient of the foundation reaction and shear stiffness of foundation can be determined using the following equations [22, 23]:

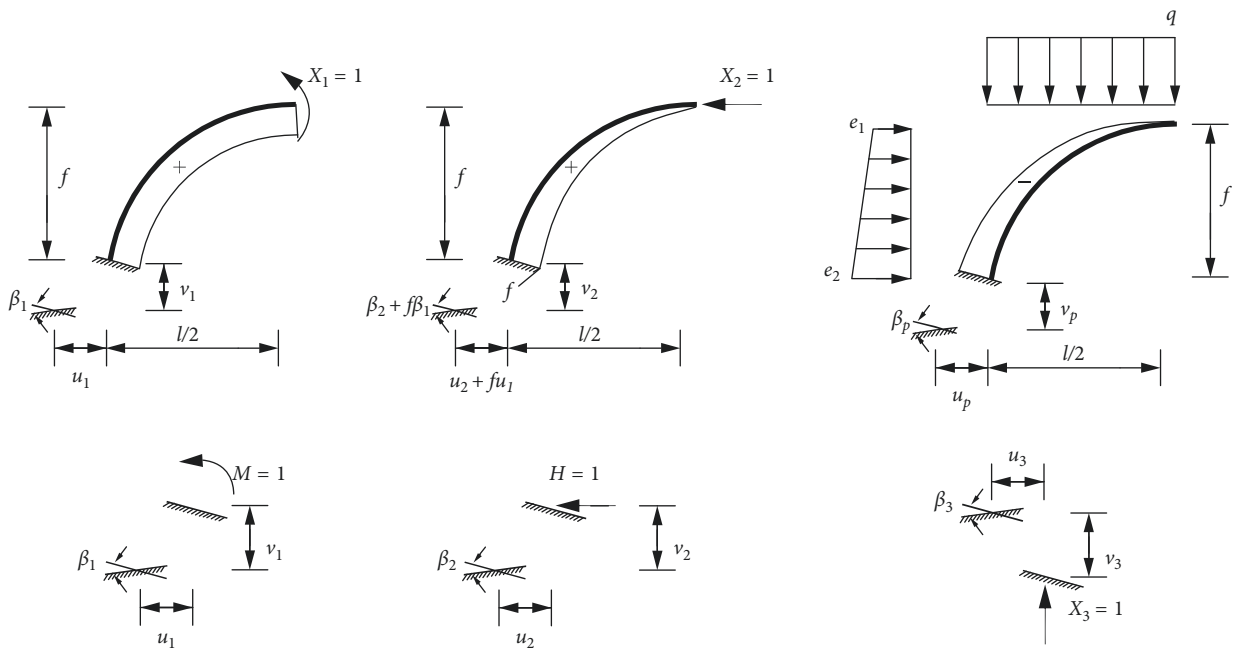

Figure 6: Displacements at the foot section of the steel rib caused by the unit forces acting at the arch foot section and crown section.

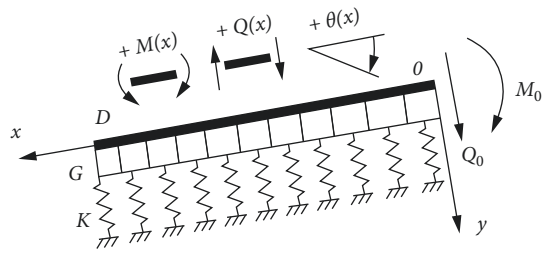

Figure 7: Mechanical model of the feet-lock pipe based on the Pasternak double-parameter foundation.

$$K = 1.3\frac{E_s}{B\left(1-\nu_s^2\right)}\left(\frac{E_sB^4}{EI}\right)^{1/12},$$
$$G = \frac{E_st}{6\left(1+\nu_s\right)}, \tag{12}$$

where E_s and ν_s are the Young's modulus (Pa) and Poisson's ratio of foundation, respectively; $EI = n(E_pI_p + E_gI_g)$ is the equivalent bending stiffness of the feet-lock pipe (N·m^2); n is the quantity of the grouted steel pipe; E_pI_p is the bending stiffness of the steel pipe cross section (N·m^2); E_gI_g is the bending stiffness of the grout cross section inside the steel pipe (N·m^2); and t is the thickness of foundation shear layer, which can be estimated as $11B$ [24].

The differential equation of the deflection of the feet-lock pipe on the Pasternak model in the two-dimensional plane strain condition is expressed as

$$EI\frac{d^4y(x)}{dx^4} - GB\frac{d^2y(x)}{dx^2} + KBy(x) = 0. \tag{13}$$

In practice, $\rho < 1$, i.e., $G_p\alpha^2/K < 1$, where $\alpha = \sqrt[4]{KB/4EI}$; the solution of equation (13) can be expressed as follows:

$$y(x) = e^{\alpha_1\alpha x}\left(C_1\cos\left(\alpha_2\alpha x\right) + C_2\sin\left(\alpha_2\alpha x\right)\right) + e^{-\alpha_1\alpha x}\left(C_3\cos\left(\alpha_2\alpha x\right) + C_4\sin\left(\alpha_2\alpha x\right)\right), \tag{14}$$

where

$$\alpha_1 = \left[1 + \left(G_p\alpha^2\right)/K\right]^{1/2},$$
$$\alpha_2 = \left[1 - \left(G_p\alpha^2\right)/K\right]^{1/2}. \tag{15}$$

$C1$~$C4$ are integration constants that can be determined by the boundary conditions at the near-end and far-end of the feet-lock pipe.

Using boundary conditions at the far-end of the feet-lock pipe, i.e., $y(x)|_{x\longrightarrow\infty} = 0$ and $\theta(x)|_{x\longrightarrow\infty} = 0$, one can get $C1 = C2 = 0$. Besides, using the boundary condition at the near-end of the feet-lock pipe, i.e.,

$$M_x\big|_{x=0} = EI\frac{d^2y}{dx^2}\Big|_{x=0} = M_0,$$
$$Q_x\big|_{x=0} = EI\frac{d^3y}{dx^3}\Big|_{x=0} = Q_0. \tag{16}$$

The residual integration constants can be determined as equations (17) and (18):

$$C_3 = \frac{1}{EI\alpha^3\left(\alpha_1^2+\alpha_2^2\right)^2}\left[2Q_0\alpha_1 + M_0\alpha\left(3\alpha_1^2 - \alpha_2^2\right)\right], \tag{17}$$

$$C_4 = \frac{1}{EI\alpha^3\alpha_2\left(\alpha_1^2+\alpha_2^2\right)^2}\left[Q_0\left(\alpha_1^2 - \alpha_2^2\right) + M_0\alpha\alpha_1\left(\alpha_1^2 - 3\alpha_2^2\right)\right]. \tag{18}$$

Substituting the determined integration constants $C1$~$C4$ into equation (14), the deflection function of the feet-lock pipe can be expressed as

$$y(x) = \frac{e^{-\alpha_1 \alpha x}}{EI\alpha^3 \alpha_2 \left(\alpha_1^2 + \alpha_2^2\right)^2} \cdot \left\{ \left[2Q_0 \alpha_1 \alpha_2 + M_0 \alpha \alpha_2 \left(3\alpha_1^2 - \alpha_2^2\right)\right] \cos\left(\alpha_2 \alpha x\right) + \left[Q_0 \left(\alpha_1^2 - \alpha_2^2\right) + M_0 \alpha \alpha_1 \left(\alpha_1^2 - 3\alpha_2^2\right)\right] \sin\left(\alpha_2 \alpha x\right) \right\}. \tag{19}$$

Moreover, the rotation angle of the feet-lock pipe can be determined from the analytical solution of the deflection as

$$\theta(x) = -\frac{dy}{dx} = \alpha e^{-\alpha_1 \alpha x} \left[\left(\alpha_1 C_3 - \alpha_2 C_4\right) \cos\left(\alpha_2 \alpha x\right) + \left(\alpha_1 C_4 + \alpha_2 C_3\right) \sin\left(\alpha_2 \alpha x\right) \right]. \tag{20}$$

Using equations (19) and (20), the lateral displacement and rotation angle of the feet-lock pipe at its near-end can be expressed as

$$y_0 = \frac{4\alpha \left[2Q_0 \alpha_1 + M_0 \alpha \left(3\alpha_1^2 - \alpha_2^2\right)\right]}{KB\left(\alpha_1^2 + \alpha_2^2\right)^2}, \tag{21}$$

$$\theta_0 = \frac{4\alpha^2 \left[Q_0 + 2M_0 \alpha \alpha_1\right]}{KB\left(\alpha_1^2 + \alpha_2^2\right)}. \tag{22}$$

3.3. Displacements at the Arch Foot Section. After the lateral displacement and rotation angle of the feet-lock pipe at its near-end are determined as equations (21) and (22), the displacements including the horizontal displacements, vertical displacements, and rotation angles at the foot section of the steel rib needed in equation (9) can be obtained as follows:

$$\beta_1 = \frac{8\alpha^3 \alpha_1}{KB\left(\alpha_1^2 + \alpha_2^2\right)}, \tag{23}$$

$$u_1 = \frac{4\alpha^2 \left(3\alpha_1^2 - \alpha_2^2\right)}{KB\left(\alpha_1^2 + \alpha_2^2\right)^2} \sin\,\theta, \tag{24}$$

$$v_1 = -\frac{4\alpha^2 \left(3\alpha_1^2 - \alpha_2^2\right)}{KB\left(\alpha_1^2 + \alpha_2^2\right)^2} \cos\,\theta, \tag{25}$$

$$\beta_2 = \frac{4\alpha^2}{KB\left(\alpha_1^2 + \alpha_2^2\right)} \sin\,\theta, \tag{26}$$

$$u_2 = \frac{8\alpha\alpha_1}{KB\left(\alpha_1^2 + \alpha_2^2\right)^2} \sin^2\,\theta, \tag{27}$$

$$v_2 = -\frac{4\alpha\alpha_1}{KB\left(\alpha_1^2 + \alpha_2^2\right)^2} \sin\,2\theta, \tag{28}$$

$$\beta_3 = \beta_2 \cot\,\theta, \tag{29}$$

$$u_3 = u_2 \cot\,\theta, \tag{30}$$

$$v_3 = v_2 \cot\,\theta, \tag{31}$$

$$\beta_p = \frac{4\alpha^2 \left[Q_p + 2M_p \alpha \alpha_1\right]}{KB\left(\alpha_1^2 + \alpha_2^2\right)}, \tag{32}$$

$$u_p = -\frac{4\alpha \left[2Q_p \alpha_1 + M_p \alpha \left(3\alpha_1^2 - \alpha_2^2\right)\right]}{KB\left(\alpha_1^2 + \alpha_2^2\right)^2} \sin\,\theta, \tag{33}$$

$$v_p = \frac{4\alpha \left[2Q_p \alpha_1 + M_p \alpha \left(3\alpha_1^2 - \alpha_2^2\right)\right]}{KB\left(\alpha_1^2 + \alpha_2^2\right)^2} \cos\,\theta, \tag{34}$$

where θ is the installation angle of the feet-lock pipe, i.e., the angle between the horizontal line and axial line of the feet-lock pipe.

$$M_p = \frac{1}{8} ql^2 + \frac{1}{2} e_1 f^2 + \frac{1}{6} \left(e_2 - e_1\right) f^2, \qquad Q_p = \frac{1}{2} ql \cos\,\theta + \frac{1}{2} \left(e_1 + e_2\right) f \sin\,\theta. \tag{35}$$

From the above derivation, three unknown forces X_1, X_2, and X_3 shown in Figure 4 can be finally solved by substituting equations (3)–(7) and (23)–(34) into equation (9). Meanwhile, the vertical load at the foot of the steel rib can be easily obtained. Its magnitude equals to the foundation reaction X_3. The foot settlement of the steel rib with the support of the feet-lock pipe can also be estimated as follows:

$$\Delta_{\text{foot}} = X_3 / \left(K_{\text{f}} A_{\text{f}}\right). \tag{36}$$

4. Validation of the Analytical Method

In order to validate the feasibility and accuracy of the presented analytical method, the predictions of the vertical load and foot settlement of the steel rib with the support of the feet-lock pipe were compared with those obtained from field measurements in tunnel projects and the results from the Winkler model of the feet-lock pipe.

4.1. Case Study 1

4.1.1. Overview of the Tianhengshan Tunnel. The Tianhengshan tunnel, situated at the northeast of the Harbin Ring Expressway, is an up-and-down separation type tunnel project. The up line is 1660 m in length, and the down line is 1690 m in length. The effective clear width of the tunnel is 11.5 m. The effective clear height of the tunnel is 5 m. What the tunnel penetrates through the strata is mainly cohesive soil. The physical and mechanics parameters of the soil are listed in Table 1.

The partial excavation method was used to construct the tunnel, as shown in Figure 8. The numbers in Figure 8

Table 1: Physical and mechanics parameters of the soil.

Items	Soil grade	
	VI	V
Density (kg/m^3)	1960	1930
Water content (%)	26.9	27.2
Young's modulus (MPa)	6.79	10.81
Cohesion (kPa)	14.2	16.9
Friction angle (°)	27.6	26.2
Poisson's ratio	0.3	0.3

represent the excavation sequence of the tunnel. When tunneling in the ground of cohesive soil, we found that the supporting effect of the systematic rock bolt is difficult to be exerted because of its poor anchoring effect in cohesive soil ground. As a result, the rock bolt was replaced by the feet-lock pipe to stabilize the foot of the steel rib. The basic parameters of the steel rib and the feet-lock pipe are as shown in Table 2.

4.1.2. Field Monitoring. In order to examine the supporting effect of the feet-lock pipe during the tunnel construction, total station was adopted to measure the foot settlement of steel ribs. The measurements of the four cross sections (Section XK89 + 588, Section XK89 + 605, Section SK89 + 355.6, and Section SK89 + 397.6) were selected to validate the feasibility and accuracy of the presented calculation method. In these monitored sections, the sections of XK89 + 588 and XK89 + 605 have the depth of 25 m. The sections of SK89 + 397.6 and SK89 + 404 have the depth of 20 m. The measured foot settlements and vertical loads by back analysis of the settlements are given in Table 3.

4.1.3. Theoretical Prediction

(1) Estimation of earth pressure

Steel ribs in tunnels should be designed considering the cooperative work between the steel rib and shotcrete; namely, the maximum support resistance or earth pressure is determined according to the equation as

$$p = Ku, \tag{37}$$

where p is the support resistance, K is the support stiffness, and u is the support displacement. However, the limit equilibrium state between the ground deformation and support resistance is changed with the support deformation in soft cracked ground and is difficult to determine. On the contrary, the deformation of the soft cracked ground increases quickly in the early stage after tunnel excavation, which may result in larger deformation and a certain range of loosing earth pressure. Therefore, the steel rib can be designed to support the loosing earth pressure alone in its early stage [25].

For shallow tunnels such as the Tianhengshan tunnel, the earth pressure is mainly from the vertical earth pressure above the tunnel. The determination of the vertical earth pressure is a top priority for the design of the shallow tunnel. Various theoretical methods have been established to estimate the earth pressure. The formulas of Terzaghi [26], Xie [27], and Bierbaumer [28] and the method of whole earth column weight above the tunnel are the most recognized methods to calculate the loosening earth pressure of the shallow tunnels.

Figure 9 shows the comparison of vertical earth pressures with tunnel depths using the four different theoretical formulas in grade VI soil. From Figure 9, it can be seen that the classic theories of loosening earth pressure differ notably in calculated results because of different assumptions, and these differences increase obviously with the increase of tunnel buried depth. The method of whole earth column weight has the maximum of the earth pressure, which increases linearly with increasing buried depth. For tunnels with larger buried depth, this method would result in an overlarge load and uneconomical design. Terzaghi's formula has the minimum of the earth pressure, which increases gradually with increasing buried depth and tends to be stable. It is often used in soil tunnels with shallow or deep depth and widely adopted in tunnel design in Europe, America, Japan, and other countries. The earth pressure calculated by Bierbaumer's formula show a parabolic distribution with the increasing buried depth. Obviously, it is only applicable in the shallow tunnels. The earth pressure calculated by Xie Jiaxiao's formula is smaller than that from the theory of whole earth column weight, while is larger than those from the formulas of Terzaghi and Bierbaumer. Hence, the earth pressure is relatively conservative. On the contrary, Xie Jiaxiao's method that uses loose media theory is the specified calculation method of the earth pressure for shallow tunnels in China [29, 30]. In this study, Xie Jiaxiao's formula is chosen to calculate the earth pressure of the Tianhengshan tunnel.

According to Xie Jiaxiao's formula [27], the earth pressures for shallow tunnels can be calculated as follows:

$$\left.\begin{aligned} q &= \gamma H\left(1 - \left(H\lambda \tan\theta/l\right)\right) \\ e_1 &= \lambda H\gamma \\ e_2 &= \lambda\left(H + f\right)\gamma \end{aligned}\right\}, \tag{38}$$

where

$$\lambda = \frac{\tan\beta - \tan\varphi_c}{\tan\beta\left[1 + \tan\beta\left(\tan\varphi_c - \tan\theta\right) + \tan\varphi_c \tan\theta\right]},$$

$$\tan\beta = \tan\varphi_c + \sqrt{\frac{\left(\tan^2\varphi_c + 1\right)\tan\varphi_c}{\tan\varphi_c - \tan\theta}}. \tag{39}$$

γ is the unit weight of the soil (kN/m^3), H is the tunnel depth (m), θ is the friction angle beside the soil pillar (°), λ is the coefficient of lateral earth pressure, φ_c is the calculated friction angle of the soil which takes into account the effect of cohesion and friction angle (°), and β is the rupture angle between the rupture surface and the horizontal surface (°).

Using equation (38), the total earth pressures for the sections of XK89 + 588 and XK89 + 605 can be estimated

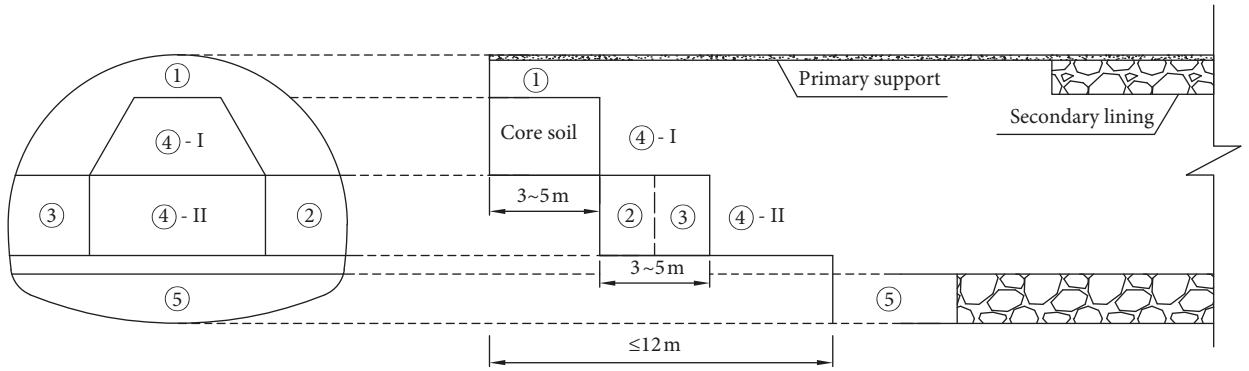

Figure 8: 2D sketch of the partial excavation method.

Table 2: Basic parameters of the steel rib and the feet-lock pipe.

Items	Soil grade	
	VI	V
Type of steel ribs	I20a	I18
Contact area at the foot of the steel rib (cm^2)	24×15	22×15
Interval of steel ribs (m)	0.5	0.75
Length of the feet-lock pipe (m)	5	4
Quantity and diameter of the feet-lock pipe at each foot (mm)	$6\Phi 42 \times 4$	
Angle of the feet-lock pipe (°)	30	
Young's modulus of steel ribs (GPa)	206	
Radius of steel ribs (m)	6.5	
Span of steel ribs (m)	11.47	
Height of steel rib (m)	3.44	
Young's modulus of the feet-lock pipe (GPa)	206	
Young's modulus of cement grout (GPa)	23	

Table 3: Field measurements of tunnel sections with the different soil grades.

Soil grade	Tunnel section	Foot settlement (mm)	Average settlement (mm)	Vertical load by back analysis (kN)
VI	XK89 + 588 XK89 + 605	18.0~21.0 16.0~17.0	18.0	45.98
V	SK89 + 355.6 SK89 + 397.6	13.2~13.4 14.0~14.8	13.9	53.68

as $q = 406.2$ kN/m, $e_1 = 154.2$ kN/m, and $e_2 = 175.4$ kN/m; the total earth pressures for the sections of SK89 + 355.6 and SK89 + 397.6 can be estimated as $q = 320.7$ kN/m, $e_1 = 102.9$ kN/m, and $e_2 = 120.6$ kN/m.

According to the experience in tunnel design and construction [25], the loosing earth pressures acted on the steel rib can be estimated as 10%~40% of the total loosing earth pressures. For grade VI of the soil, the load ratio of the steel rib can be estimated as 10% of the total loosing earth pressures. For grade V of the soil, the load ratio of the steel rib can be estimated as 15% of the total loosing earth pressures.

(2) Prediction of the foot settlement and the vertical load

Based on the above analysis of the earth pressure acted on the steel rib, the foot settlement and vertical load at the foot of the steel rib with the support of the feet-lock pipe was calculated by using equations (9) and (36). In order to obtain a better comparison, another two conditions were also performed. In one condition, the feet-lock pipe was modeled using the Winkler model, and in the other one, the feet-lock pipe is not installed at the foot of the steel rib.

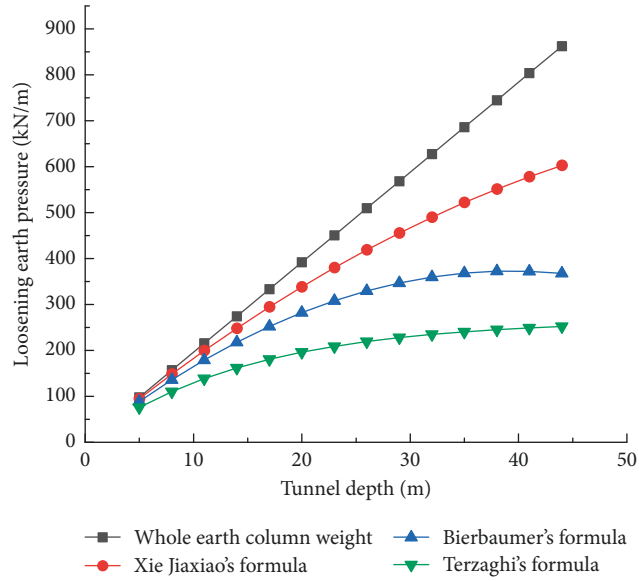

Figure 9: Comparison of vertical earth pressure with tunnel depths using four theoretical formulas in grade VI of the soil.

Table 4 shows the comparison of the predicted foot settlements. It can be seen that the predicted foot settlements using the proposed approach are a little smaller than the results from the previous model of the feet-lock pipe and are closer to the measured results. Table 5 shows the comparison of the predicted vertical loads at the foot. It can be seen that the predicted vertical loads are also a little smaller than the results from the previous model of the feet-lock pipe and closer to the vertical loads by back analysis of the measured foot settlements. In addition, the vertical loads in the cases of support with the feet-lock pipe are only about 20% of the cases without the feet-lock pipe. This illustrates the feet-lock pipe can transfer the vertical load, significantly, and have a

Table 4: Comparison of the predicted foot settlements.

Soil grade	Tunnel section	Average foot settlement (mm)	Proposed approach (Pasternak model) (mm)	Previous approach (Winkler model) (mm)
VI	XK89 + 588 XK89 + 605	18.0	18.9	19.2
V	SK89 + 355.6 SK89 + 397.6	13.9	14.4	14.8

Table 5: Comparison of the predicted vertical loads.

Soil grade	Tunnel section	Back analysis (kN)	Support with the feet-lock pipe (kN)		Support without the feet-lock pipe (kN)
			Pasternak model	Winkler model	
VI	XK89 + 588 XK89 + 605	45.98	48.16	48.94	232.96
V	SK89 + 355.6 SK89 + 397.6	53.68	55.86	57.16	275.88

critical role in ensuring the stability of the ground at the foot of the steel rib.

4.2. Case Study 2

4.2.1. Overview of the Jianzicha Tunnel 2. The Jianzicha tunnel 2 is situated on the highway from Huangling to Yanan in China. It is a 3-lane tunnel through the loess ground. The unit weight of loess is 16.5 kN/m^3, the water content of loess is 15%~17%, the young's modulus is 20 MPa, the Poisson's ration is 0.37, the cohesion is 20 kPa, and the friction angle is 26°. The maximum depth of the tunnel is 94 m. The left line of the tunnel is 555 m in length, and the right line of the tunnel is 365 m in length. The effective clear width of the tunnel is 14.5 m, and the effective clear height of the tunnel is 5 m. To decrease the disturbance to the surrounding rock, the tunnel was excavated by using the partial excavation method. The basic parameters for the excavation and primary support are listed in Table 6.

4.2.2. Comparison of Measurement and Prediction. During the tunnel construction, the earth pressures acting on the steel rib and the settlements at the foot of the steel rib were monitored. According to the measured results of the earth pressures acting on the steel rib, the vertical earth pressure q was 0.032~0.052 MPa, the lateral earth pressure e_2 was 0.026~0.04 MPa, and the lateral earth pressure was $e_1 = 0.005$~0.012 MPa. According to the measured results of the cross sections ZK80 + 945, ZK80 + 950, ZK80 + 955, ZK80 + 960, ZK80 + 970, ZK80 + 975, and ZK80 + 980, the settlements at the feet of the steel ribs were 11~18 mm. The vertical loads at the feet of the steel ribs were 115.25~188.58 KN.

Using the proposed analytical method, the predicted settlements at the feet of the steel ribs are 11.21~18.22 mm, and the predicted vertical loads at the feet are 117.41~190.96 kN. Compared with the measured results, the predicted values have a very small prediction error and agrees well with the measured results.

Table 6: Basic parameters for excavation and support of the tunnel.

Items	Value
Type of steel ribs	I25a
Contact area at the foot of the steel rib (cm^2)	26 × 18
Interval of steel ribs (m)	0.6
Length of the feet-lock pipe (m)	5
Quantity and diameter of the feet-lock pipe at each foot	2Φ50 mm × 4 mm
Angle of the feet-lock pipe (°)	20°
Young's modulus of steel ribs (GPa)	206
Radius of steel ribs (m)	8.66
Span of steel ribs (m)	17.06
Height of steel ribs (m)	7.15
Young's modulus of the feet-lock pipe (GPa)	206
Young's modulus of cement grout (GPa)	23

Based on the above comparison and analysis, it can be proved that the presented method is feasible to predict the vertical load and settlement at the foot of the steel rib with the support of the feet-lock pipe, and the discrepancy is acceptable. By using the presented method, the ground stability at the foot of the steel rib with the support of the feet-lock pipe can be quantitatively evaluated.

5. Conclusions

In order to predict the vertical load and settlement at the foot of the steel rib with the support of the feet-lock pipe, an analytical method was proposed based on the mechanical model of the steel rib and the feet-lock pipe combined structure. In this method, the deformation compatibility among the steel rib, the feet-lock pipe, and the ground at the foot were considered, and an elastic foundation beam model with double parameter for the feet-lock pipe was proposed to reflect the shear resistance of the ground. Based on the developed mechanical model, the analytical equations for predicting the vertical load and settlement at the foot were derived using structural analysis and beam theory on elastic foundation. The predicted vertical loads and foot settlements

were validated by comparing with the results of field measurements and existing mechanical model. Besides, it was found that the vertical load in tunnel support with the feet-lock pipe is only about 20% of than that in tunnel support without the feet-lock pipe. This illustrated the feet-lock pipe can effectively reduce the load acting on the ground where the steel rib was set and help improve the stability of tunnel structure.

Data Availability

The measured data used to support the findings of this study are included within the article such as the foot settlements in case study 1 and case study 2 and the measured earth pressures in case study 2. Using the measured data, supporting parameters in the case studies, and the derived formula in this article, researchers can verify the results of the article, replicate the analysis, and conduct secondary analyses.

Conflicts of Interest

The authors declare that they have no conflicts of interest.

Acknowledgments

The authors gratefully acknowledge the financial support by the National Natural Science Fund Project of China (nos. 41831286 and 51808049) and the Changjiang Scholar Program of Chinese Ministry of Education (Grant no. T2014214).

References

[1] M. Miwa and M. Ogasawara, "Tunnelling through an embankment using all ground fasten method," *Tunnelling and Underground Space Technology*, vol. 20, no. 2, pp. 121–127, 2005.

[2] Y. Cui, M. Kimura, and M. Nonomura, "Control of surface settlement arising from the phenomenon of accompanied settlement using foot reinforcement side pile," in *Proceedings of ITA-AITES World Tunnel Congress*, Budapest, Hungary, May 2009.

[3] Y. Cui and M. Kimura, "Analytical study on the control of ground subsidence arising from the phenomenon of accompanied settlement using foot reinforcement side pile," in *Deep and Underground Excavation*, pp. 307–312, ASCE Geotechnical Special Publication, Reston, VA, USA, 2010.

[4] K. Haruyama, K. Taira, and K. Tanaka, "Evaluation of measure taken for controlling subsidence for a large-scale double deck tunnel at shallow depth," *Proceedings of IS-Kyoto*, vol. 2, pp. 769–774, 2001.

[5] E. Leca, "Settlements induced by tunneling in soft ground," *Tunnelling and Underground Space Technology*, vol. 22, no. 2, pp. 119–149, 2007.

[6] K. Miura, "Design and construction of mountain tunnels in Japan," *Tunnelling and Underground Space Technology*, vol. 18, no. 2-3, pp. 115–126, 2003.

[7] H. Kimura, T. Itoh, M. Iwata, and K. Fujimoto, "Application of new urban tunneling method in Baikoh tunnel excavation," *Tunnelling and Underground Space Technology*, vol. 20, no. 2, pp. 151–158, 2005.

[8] Q. Fang, D. Zhang, and L. N. Y. Wong, "Shallow tunnelling method (STM) for subway station construction in soft ground," *Tunnelling and Underground Space Technology*, vol. 29, no. 3, pp. 10–30, 2012.

[9] Q. Fang, D. Zhang, Q. Li, and L. N. Y. Wong, "Effects of twin tunnels construction beneath existing shield-driven twin tunnels," *Tunnelling and Underground Space Technology*, vol. 45, pp. 128–137, 2015.

[10] P. F. Li, Y. Zhao, and X. J. Zhou, "Displacement characteristics of high-speed railway tunnel construction in loess ground by using multi-step excavation method," *Tunnelling and Underground Space Technology*, vol. 51, pp. 41–55, 2015.

[11] L. J. Chen, Y. L. Zhang, and Z. Y. Ma, "Analytical approach for support mechanism of feet-lock pipe combined with steel frame in weak rock tunnels," *KSCE Journal of Civil Engineering*, vol. 20, no. 7, pp. 2965–2980, 2016.

[12] Y. Luo, J. Chen, P. Huang, M. Tang, X. Qiao, and Q. Liu, "Deformation and mechanical model of temporary support sidewall in tunnel cutting partial section," *Tunnelling and Underground Space Technology*, vol. 61, pp. 40–49, 2017.

[13] Y. Luo, J. Chen, Y. Chen, P. Diao, and X. Qiao, "Longitudinal deformation profile of a tunnel in weak rock mass by using the back analysis method," *Tunnelling and Underground Space Technology*, vol. 71, pp. 478–493, 2018.

[14] C. Yui, K. Kishida, and M. Kimura, "Experimental study on effect of auxiliary methods for simultaneous settlement at subsurface and surface during shallow overburden tunnel excavation," *Japanese Geotechnical Journal*, vol. 3, no. 3, pp. 261–272, 2008.

[15] T. Kitagawa, M. Goto, T. Tamura et al., "Experimental studies on tunnel settlement reduction effect of side piles," *Doboku Gakkai Ronbunshuu F*, vol. 65, no. 1, pp. 73–83, 2009.

[16] Y. B. Luo and J. X. Chen, "Mechanical characteristics and mechanical calculation model of tunnel feet-lock bolt in weak surrounding rock," *Chinese Journal of Geotechnical Engineering*, vol. 35, no. 8, pp. 1519–1525, 2013.

[17] Y. Cui, K. Kishida, and M. Kimura, "Prevention of the ground subsidence by using the foot reinforcement side pile during the shallow overburden tunnel excavation in unconsolidated ground," *Tunnelling and Underground Space Technology*, vol. 63, pp. 194–204, 2017.

[18] T. Kitagawa, M. Goto, T. Tamura et al., "Numerical analyses of tunnel settlement reduction effect by side piles," *Doboku Gakkai Ronbunshuu F*, vol. 66, no. 1, pp. 85–100, 2010.

[19] Y. M. Wu, K. C. Lü, and Y. Xu, "Bearing behaviors of steel foot pipes for tunnels in soft foundation," *Chinese Journal of Geotechnical Engineering*, vol. 31, no. 12, pp. 1825–1832, 2009.

[20] Y. Tan, C. H. Shi, L. M. Peng, C. Y. Cao, and D. B. Du, "Study on the bearing capacity at arch foot of shallow buried soft base tunnel with partial excavation," *Railway Standard Design*, vol. 59, no. 2, pp. 76–81, 2015.

[21] P. L. Pasternak, *On a New Method of Analysis of an Elastic Foundation by Means of Two Foundation Constants*, Gosudarstvennoe Izdatelstvo Literaturi po Stroitelstvu i Arkhitekture, Moscow, Russia, 1954.

[22] A. J. Francis, "Analysis of pile groups with flexural resistance," *Journal of the Soil Mechanics and Foundations Division*, vol. 90, pp. 10–32, 1964.

[23] H. Tanahashi, "Formulas for an infinitely long Bernoulli-Euler beam on the Pasternak model," *Soils and Foundations*, vol. 44, no. 5, pp. 109–118, 2004.

[24] W.-J. Yao, W.-X. Yin, J. Chen, and Y.-Z. Qiu, "Numerical simulation and study for super-long pile group under axis and lateral loads," *Advances in Structural Engineering*, vol. 13, no. 6, pp. 1139–1151, 2016.
[25] Y. Q. Zhu, *Tunnel Engineering*, China Planning Press, Beijing, China, 2015.
[26] K. Terzaghi, *Rock Defects and Load on Tunnel Supports, Rock Tunnelling with Steel Support*, R. V. Proctor and T. L. White, Eds., Commercial Shearing and Stamping Co., Youngstava, OH, USA, 1946.
[27] J. X. Xie, "Earth pressure on shallow buried tunnel," *China Civil Engineering Journal*, vol. 10, no. 6, pp. 58–70, 1964.
[28] A. Bierbaumer, *Die Dimensionierung des Tunnelmauerwerks*, Engelmann, Leipzig, Germany, 1913.
[29] JTG D70-2004, *Code for Design of Road Tunnel*, China Communications Press, Beijing, China, 2004.
[30] TB 10003-2016, *Code for Design of Railway Tunnel*, China Communications Press, Beijing, China, 2016.